PHILOSOPHICAL TRANSACTIONS A

rsta.royalsocietypublishing.org

Research

Article submitted to journal

Subject Areas:
applied mathematics, mechanics

Keywords:
Rayleigh wave, thin coating, contrast, clamped surface, asymptotic

Author for correspondence:
Julius Kaplunov
e-mail: j.kaplunov@keele.ac.uk

THE ROYAL SOCIETY PUBLISHING

Rayleigh-type waves on a coated elastic half-space with a clamped surface

J. Kaplunov[1], D. Prikazchikov[1], L. Sultanova[1,2]

[1] School of Computing and Mathematics, Keele University, Keele, Staffordshire, ST5 5BG, UK
[2] International Institute for Nanocomposites Manufacturing, WMG, University of Warwick, CV4 7AL, UK

Elastodynamics of a half-space coated by a thin soft layer with a clamped upper face is considered. The focus is on the analysis of localised waves that do not exist on a clamped homogeneous half-space. Non-traditional effective boundary conditions along the substrate surface incorporating the effect of the coating are derived using a long-wave high-frequency procedure. The derived conditions are implemented within the framework of the earlier developed specialised formulation for surface waves, resulting in a perturbation of the shortened equation of surface motion in the form of an integral or pseudo-differential operator. Non-uniform asymptotic formula for the speeds of the sought for Rayleigh-type waves, failing near zero frequency and the thickness resonances of a layer with both clamped faces, follow from the aforementioned perturbed equation. Asymptotic results are compared with the numerical solutions of the full dispersion relation for a clamped coated half-space. A similarity with Love-type waves proves to be useful for interpreting numerical data.

1. Introduction

It is well known that the Rayleigh wave on a homogeneous elastic half-space [31] exists only for a traction-free surface. However, this is not the case of a layered half-space, for which the rigorous mathematical treatment in [8] demonstrates a possibility of localised waves for a clamped surface as well. In this paper we illustrate the considerations in [8] by the example of a coated half-space with a clamped surface, modelling an

interface between rigid and deformable media. The main focus is on a physical insight into the peculiarities of the observed localised dynamic phenomena using an asymptotic approach oriented to a soft coating with a stiffness much lower than that of a substrate. In this case we should expect that the associated counterparts of the Rayleigh wave could be treated as its perturbations.

The effect of a thin coating, for which a typical wave length is much greater than its thickness, may be incorporated through the so-called effective boundary conditions along the surface of a substrate. In contrast to traditional derivations usually dealing with low-frequency vibrations (the frequency range of interest is well below the first thickness resonance) of a coating with a traction-free upper face, e.g. see [10,36–38], we develop an asymptotic procedure also covering the high-frequency vibrations, similarly to what has been done for a thin interfacial layer in [17], and earlier for thin walled structures in [14,16,27], see also [4–6,18,25]. As a result, we are able to tackle higher-order Rayleigh-type waves with a sinusoidal variation across the thickness of the coating, which is a feature of a soft coating only. Indeed, without such a contrast, the long waves always propagate over the interior. It is worth noting that the coefficients in the simplest effective conditions exploited in the paper are frequency-dependent, tending to infinity at the thickness resonances of an elastic layer with both clamped faces [14]. However, this does not happen with the associated refined high-frequency conditions, see e.g. [17] for further detail.

The effective boundary conditions can be then used to proceed with a specialised hyperbolic-elliptic formulation for the studied Rayleigh-type waves, which was originally established in [15] using the symbolic Lourier approach, see e.g. [16] and references therein, and further developed in [21] starting from a slow time perturbation of the eigensolution for a homogeneous surface wave of arbitrary profile, see [7] and also earlier publications [13,35], as well as more recent papers including [1,22–24,28–30,33]. The general asymptotic methodology of extracting the contributions of surface, interfacial and edge waves from overall dynamic responses induced by prescribed loads is exposed in [19], with the effect of anisotropy addressed recently in [26]. For the basic setup of an elastic half-space subject to surface stresses, the aforementioned formulation involves a hyperbolic equation that governs propagation of surface disturbances along with pseudo-static elliptic equations over the interior. A similar methodology is also adapted for the conventional problem for a coated half-space [10], for which the hyperbolic equation along the surface is singularly perturbed by a pseudo-differential operator. The formulation has also been developed for mixed boundary value problems, suggesting a prospective approach for problems of crack propagation, see [34].

The asymptotic formulae for the corrections to the Rayleigh wave speed due to the effect of a soft coating readily follow from the pseudo-differential equation along the substrate surface. They obviously fail near zero frequency, where the localised wave is not yet generated, and in the vicinities of the thickness resonances in [14], as also may be observed from numerical comparison with the exact dispersion relation, which is also studied in great detail making use of the analogy with better understood Love-type waves.

2. Statement of the problem

Consider plane problem in linear elasticity for a half-space $(x_2 \geqslant 0)$ coated by a layer of thickness h, with a clamped surface $(-h \leqslant x_2 \leqslant 0)$, see Figure 1. In what follows, the quantities associated with the coating and the half-space are denoted with the superscripts "$-$" and "$+$", respectively.

The conventional equations of motion can be taken as, see e.g. [2],

$$\sigma^{\pm}_{i1,1} + \sigma^{\pm}_{i2,2} = \rho^{\pm} u^{\pm}_{i,tt}, \tag{2.1}$$

where $\sigma^{\pm}_{ij}$ are Cauchy stresses $(i,j=1,2)$, $u^{\pm}_{i}$ are displacements, $\rho^{\pm}$ denote volume mass densities, and comma indicates differentiation.

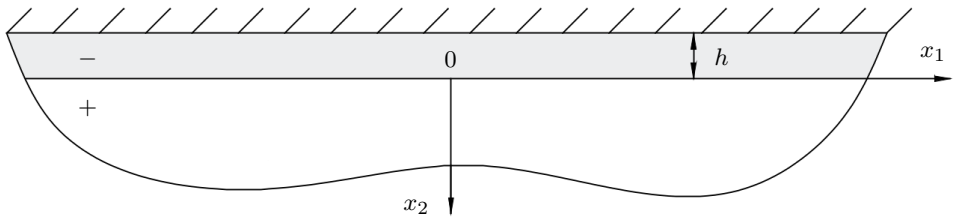

Figure 1. A clamped coated half-space

The constitutive relations in linear isotropic elasticity are adopted in the form

$$\sigma_{ij}^{\pm} = \lambda^{\pm}\delta_{ij}(u_{1,1}^{\pm} + u_{2,2}^{\pm}) + \mu^{\pm}(u_{i,j}^{\pm} + u_{j,i}^{\pm}), \tag{2.2}$$

where $\lambda^{\pm}$ and $\mu^{\pm}$ are Lamé elastic constants, and δ_{ij} is the Kronecker delta.

The boundary condition modelling a clamped surface can be written as

$$u_i^{-}\big|_{x_2=-h} = 0. \tag{2.3}$$

We also impose the continuity conditions at the interface

$$u_i^{-}\big|_{x_2=0} = u_i^{+}\big|_{x_2=0}, \qquad \sigma_{i2}^{-}\big|_{x_2=0} = \sigma_{i2}^{+}\big|_{x_2=0} \tag{2.4}$$

and assume spacial decay of displacements, i.e. $u_i^{+} \to 0$ as $x_2 \to \infty$. We usually suppose that the layer is softer than the half-space, employing, therefore, a small contrast parameter given by

$$\mu = \frac{\mu^{-}}{\mu^{+}}. \tag{2.5}$$

The displacement field can be decomposed according to the Helmholtz theorem [2] as

$$u_1^{\pm} = \varphi_{,1}^{\pm} - \psi_{,2}^{\pm}, \qquad u_2^{\pm} = \varphi_{,2}^{\pm} + \psi_{,1}^{\pm}, \tag{2.6}$$

where $\varphi^{\pm}$ and $\psi^{\pm}$ are longitudinal and transverse elastic potentials, respectively. Substituting the last formulae into the equations of motion (2.1), we arrive at the following wave equations

$$(c_1^{\pm})^2\Delta\varphi^{\pm} - \varphi_{,tt}^{\pm} = 0, \qquad (c_2^{\pm})^2\Delta\psi^{\pm} - \psi_{,tt}^{\pm} = 0, \tag{2.7}$$

where

$$c_1^{\pm} = \sqrt{\frac{\lambda^{\pm} + 2\mu^{\pm}}{\rho^{\pm}}}, \qquad c_2^{\pm} = \sqrt{\frac{\mu^{\pm}}{\rho^{\pm}}} \tag{2.8}$$

are longitudinal and transverse wave speeds, respectively, and $\Delta = \dfrac{\partial^2}{\partial x_1^2} + \dfrac{\partial^2}{\partial x_2^2}$.

The wave potentials satisfying (2.7) are found in the form of travelling harmonic waves as

$$\begin{aligned} \varphi^{-} &= [A_1\cos(\alpha^{-}kx_2) + A_2\sin(\alpha^{-}kx_2)]\mathrm{e}^{ik(x_1-ct)}, & \varphi^{+} &= A_5\mathrm{e}^{ik(x_1-ct)-\alpha^{+}kx_2}, \\ \psi^{-} &= [A_3\cos(\beta^{-}kx_2) + A_4\sin(\beta^{-}kx_2)]\mathrm{e}^{ik(x_1-ct)}, & \psi^{+} &= A_6\mathrm{e}^{ik(x_1-ct)-\beta^{+}kx_2}, \end{aligned} \tag{2.9}$$

where k is wave number, c is phase speed, A_n, $n = 1, \ldots, 6$, are arbitrary constants, and the coefficients $\alpha^{\pm}$ and $\beta^{\pm}$ are given by

$$\alpha^{-} = \sqrt{\frac{c}{(c_1^{-})^2} - 1}, \quad \beta^{-} = \sqrt{\frac{c}{(c_2^{-})^2} - 1}, \tag{2.10}$$

and

$$\alpha^{+} = \sqrt{1 - \frac{c^2}{(c_1^{+})^2}}, \qquad \beta^{+} = \sqrt{1 - \frac{c^2}{(c_2^{+})^2}}. \tag{2.11}$$

Substituting (2.9) into (2.6) and (2.2), and then satisfying boundary and continuity conditions (2.3) and (2.4), we obtain a dispersion relation in the form

$$\det\mathbf{A}=0, \tag{2.12}$$

with the following non-zero components of matrix $\mathbf{A}$

$$\begin{array}{llll} a_{11}=-ic_\alpha^-, & a_{12}=is_\alpha^-, & a_{13}=\beta^- s_\beta^-, & a_{14}=\beta^- c_\beta^-, \\ a_{21}=\alpha^- s_\alpha^-, & a_{22}=\alpha^- c_\alpha^-, & a_{23}=ic_\beta^-, & a_{24}=-is_\beta^-, \\ a_{34}=-\beta^-, & a_{36}=-\beta^+, & a_{42}=\alpha^-, & a_{45}=\alpha^+, \\ a_{51}=\mu\eta^-, & a_{54}=2i\beta^-\mu, & a_{55}=-\eta^+, & a_{56}=2i\beta^+, \\ a_{62}=2i\alpha^-\mu & a_{63}=-\mu\chi_\beta^-, & a_{65}=2i\alpha^+, & a_{66}=\chi_\beta^+, \end{array} \tag{2.13}$$

and

$$a_{31}=-a_{35}=a_{43}=-a_{46}=i. \tag{2.14}$$

In above,

$$\begin{array}{lll} s_\alpha^-=\sin(kh\alpha^-), & c_\alpha^-=\cos(kh\alpha^-), & s_\beta^-=\sin(kh\beta^-), \\ c_\beta^-=\cos(kh\beta^-), & \chi_\alpha^\pm=1\mp(\alpha^\pm)^2, & \chi_\beta^\pm=1\pm(\beta^\pm)^2, \\ \eta^\pm=2-\chi_\alpha^\pm(\kappa^\pm)^2, & & \end{array} \tag{2.15}$$

where

$$\kappa^\pm=\frac{c_1^\pm}{c_2^\pm}=\sqrt{\frac{2-2\nu^\pm}{1-2\nu^\pm}}, \tag{2.16}$$

with $\nu^\pm$ denoting Poisson's ratios.

It may be easily verified that the dispersion relation (2.12) for a homogeneous half-space, i.e. when $\mu^-=\mu^+$, $\lambda^-=\lambda^+$ and $\rho^-=\rho^+$, has no solutions due to boundary condition (2.3) along the clamped surface. Our goal is to demonstrate that the presence of inhomogeneity in the form of a coating supports a family of solutions, corresponding to Rayleigh-type surface waves, as follows from the mathematical analysis in [8]. Prior to interpreting these waves as a perturbation of the classical Rayleigh waves [31] in terms of a small contrast parameter μ, we investigate the dispersion relation (2.12) numerically.

3. Numerical analysis of the dispersion relation

In this section we present numerical results for the dispersion relation (2.12). They are interpreted starting from a similarity with Love-type waves discussed in the Appendix A. Below we analyse the effect of the relative stiffness μ, defined by (2.5), setting

$$\nu^-=0.3, \qquad \nu^+=0.25, \qquad \text{and} \qquad \rho=\frac{\rho^-}{\rho^+}=0.6. \tag{3.1}$$

As Love-type waves, see explicit formulae (A.7), the localised waves of interest seemingly exist under the condition

$$\frac{\mu^-}{\mu^+}=\mu<\rho=\frac{\rho^-}{\rho^+}, \quad \text{or} \quad c_2^-<c_2^+. \tag{3.2}$$

This is in agreement with Figure 2, in which $\rho=0.6$, and $\mu=0.3$ and $\mu=0.5$, and blue solid lines depict dispersion curves (2.12), yellow and green dashed lines represent the shear wave speeds

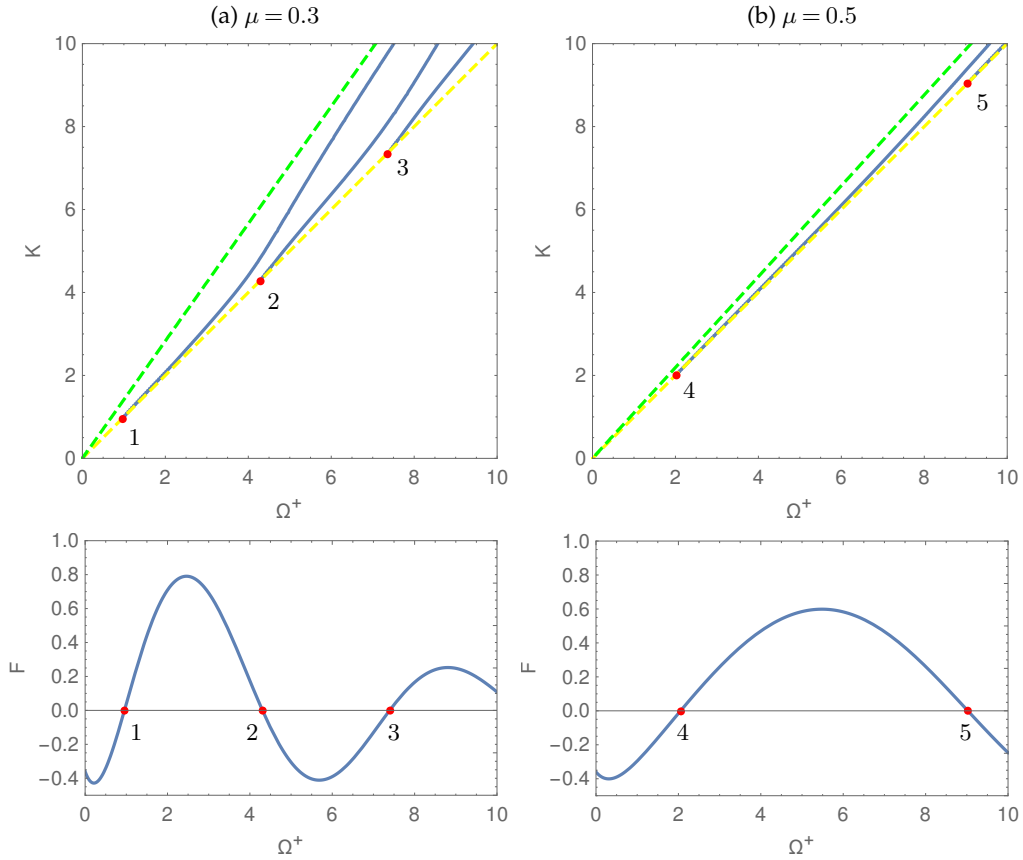

Figure 2. Dispersion curves for Rayleigh-type waves and associated functions $F(\Omega^+)$.

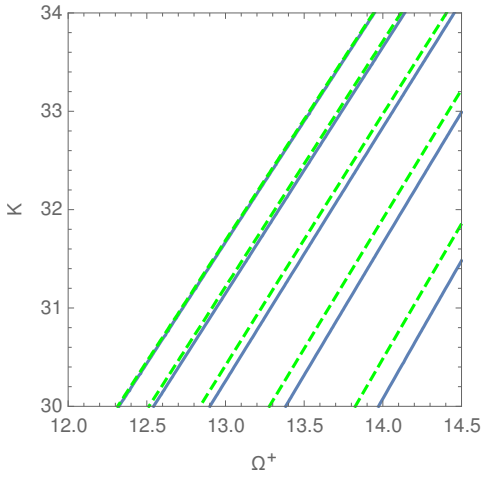

Figure 3. Short-wave behaviour of Rayleigh-type waves at $\mu = 0.1$.

of the substrate $c = c_2^+$ and the coating $c = c_2^-$, respectively, and also

$$\Omega^+ = \frac{\omega h}{c_2^+}, \qquad K = kh, \tag{3.3}$$

and

$$F(\Omega^+) = \det\mathbf{A}|_{c=c_2^+}\,. \tag{3.4}$$

This function is the result of the substitution of $c = c_2^+$ into the dispersion relation (2.12). Similarly to the explicit formula (A.7), the transcendental equation $F(\Omega^+) = 0$ determines the cut-off frequencies marked as red dots numbered from 1 to 5 in Figure 2.

Short-wave approximations of (2.12) at $K \gg 1$ are identical to those for the Love-type waves, see (A.8). Numerical comparison at $\mu = 0.1$ is shown in Figure 3, where blue solid and green dashed lines correspond to (2.12) and (A.8), respectively.

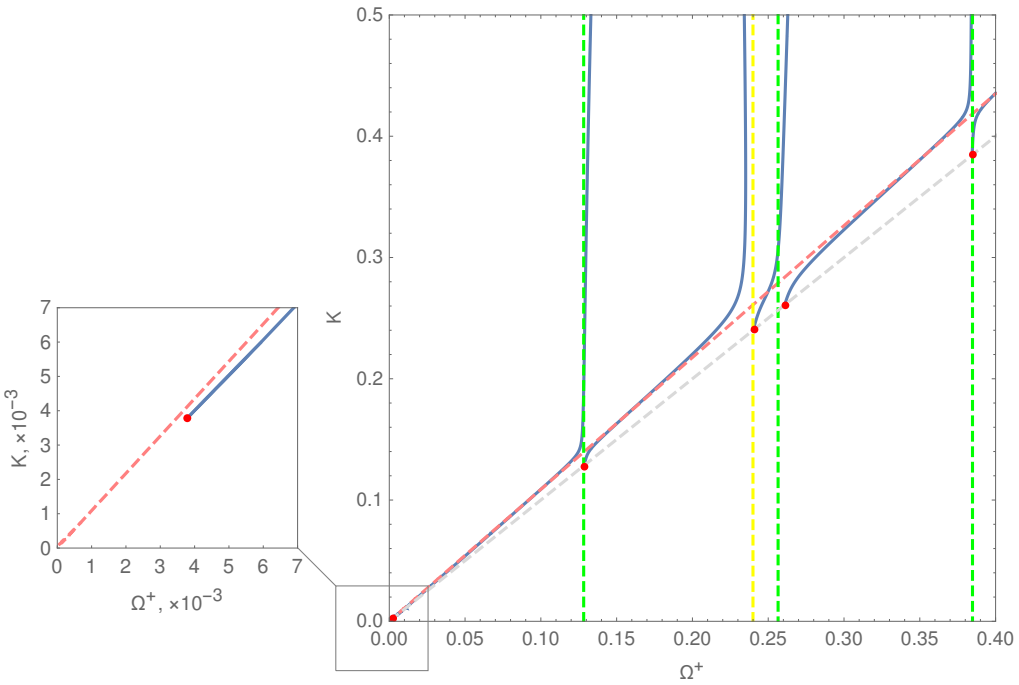

Figure 4. Dispersion curves for Rayleigh-type waves for high-contrast setup ($\mu = 0.001$).

If contrast in stiffness of the layer and the half-space is substantial, the Rayleigh wave limit gives a reasonably accurate approximation, except for the vicinities of certain thickness resonances, as well as near-zero frequency, see Figure 4, in which $\mu = 0.001$. In this Figure, blue curves correspond to the dispersion relation (2.12), the origins of the modes, denoted as red dots, are located on the dashed grey line $\Omega^+ = K$, associated with the shear wave speed of the substrate $c = c_2^+$, a pink dashed line represents the Rayleigh wave limit $c = c_R$, and yellow and green dashed lines are for stretch and shear thickness resonance frequencies, respectively. The latter are expressed as

$$\Omega^+_{st} = \sqrt{\frac{\mu}{\rho}}\kappa^-\pi n, \qquad \Omega^+_{sh} = \sqrt{\frac{\mu}{\rho}}\pi n, \qquad n = 1, 2, 3, \dots\,. \tag{3.5}$$

These are the eigenvalues of the 1D problem along the cross section of the layer with clamped faces, given by

$$h^2 u^-_{1,22} + \left(\Omega^+\sqrt{\frac{\rho}{\mu}}\right)^2 u^-_1 = 0, \qquad h^2 u^-_{2,22} + \left(\frac{\Omega^+}{\kappa^-}\sqrt{\frac{\rho}{\mu}}\right)^2 u^-_2 = 0, \tag{3.6}$$

subject to

$$u_i^-\big|_{x_2=-h} = u_i^-\big|_{x_2=0} = 0. \tag{3.7}$$

It is seen from Figure 2 that as the contrast grows (from $\mu = 0.5$ to $\mu = 0.3$), the density of the cut-off frequencies seemingly increases. Moreover, high contrast ($\mu \ll 1$) necessitates the lowest cut-off frequency becoming small, as seen on a zoomed part of Figure 4 showing the behavior of the first mode in the near-zero vicinity. This phenomenon has been recently noted in studies of low-frequency dynamics in high-contrast elastic composites, see e.g. [20]. We also observe that the dispersion curves in Figure 4 look similar to those for seismic metasurfaces, see e.g. [9,11].

The fact that the Rayleigh wave is very pronounced in case of a high contrast, i.e. it provides a good approximation for a broad range of frequencies, inspires approaching the original problem in plane elasticity in Section 2 within the framework of the hyperbolic-elliptic model for the near-surface wave field [19], see Appendix B. However, before implementing this model, we try to reduce the role of the coating to effective boundary conditions along the interface $x_2 = 0$ as has been done, for example, in [10] dealing with a layered half-space subject to normal stress applied along the surface.

4. Effective boundary conditions

Consider an inhomogeneous Dirichlet problem for an infinite thin layer ($-h \le x_2 \le 0$), subject to the boundary conditions

$$u_i^-\big|_{x_2=-h} = 0, \qquad u_i^-\big|_{x_2=0} = v_i, \tag{4.1}$$

where $v_i(x_1, x_2)$ are prescribed displacements.

First, introduce the dimensionless coordinates and frequency by

$$\xi_1 = \frac{x_1}{l}, \qquad \xi_2 = \frac{x_2 + h}{h}, \qquad \text{and} \qquad \Omega^- = \frac{\omega h}{c_2^-}, \tag{4.2}$$

where l is a typical wave length, which is assumed to be much greater than the thickness h, i.e.

$$\varepsilon = \frac{h}{l} \ll 1. \tag{4.3}$$

Let us adapt a long-wave asymptotic procedure, see e.g. [16], setting

$$u_i^- = h u_i^{*-}, \qquad \sigma_{ii}^- = \mu^- \sigma_{ii}^{*-}, \qquad \sigma_{12}^- = \mu^- \sigma_{12}^{*-}, \qquad v_i = h v_i^*, \tag{4.4}$$

where the quantities with an asterisk are of order unity.

In this case, we make an important assumption

$$\Omega^- \lesssim 1, \tag{4.5}$$

which includes the so-called high-frequency long-wave approximations, e.g. see [16]. Before, the effective boundary conditions were usually known for the small frequencies ($\Omega^- \ll 1$), enabling analysis of the low-frequency Rayleigh-type waves only. In this paper, assuming $\Omega^- \sim 1$, we are able to tackle high-frequency surface waves as well.

In view of the formulae above in this section, the equations (2.1) and (2.2) become

$$\begin{aligned}
&\varepsilon \sigma_{i1,1}^{*-} + \sigma_{i2,2}^{*-} + (\Omega^-)^2 u_i^{*-} = 0,\\
&\sigma_{11}^{*-} = \varepsilon (\kappa^-)^2 u_{1,1}^{*-} + \left((\kappa^-)^2 - 2\right) u_{2,2}^{*-},\\
&\sigma_{22}^{*-} = \varepsilon \left((\kappa^-)^2 - 2\right) u_{1,1}^{*-} + (\kappa^-)^2 u_{2,2}^{*-},\\
&\sigma_{12}^{*-} = u_{1,2}^{*-} + \varepsilon u_{2,1}^{*-},
\end{aligned} \tag{4.6}$$

subject to boundary conditions (4.1) rewritten as

$$u_i^{*-}\big|_{\xi_2=0} = 0, \qquad u_i^{*-}\big|_{\xi_2=1} = v_i^*, \tag{4.7}$$

with $v_i^* = v_i/h$. We expand the scaled displacements and stresses in asymptotic series as

$$\begin{pmatrix} u_i^{*-} \\ \sigma_{ii}^{*-} \\ \sigma_{12}^{*-} \end{pmatrix} = \begin{pmatrix} u_i^{-(0)} \\ \sigma_{ii}^{-(0)} \\ \sigma_{12}^{-(0)} \end{pmatrix} + \varepsilon \begin{pmatrix} u_i^{-(1)} \\ \sigma_{ii}^{-(1)} \\ \sigma_{12}^{-(1)} \end{pmatrix} + \dots . \tag{4.8}$$

At leading order, we have

$$\begin{aligned} &\sigma_{i2,2}^{-(0)} + (\Omega^-)^2 u_i^{-(0)} = 0, \\ &\sigma_{11}^{-(0)} = \left((\kappa^-)^2 - 2\right) u_{2,2}^{-(0)}, \\ &\sigma_{22}^{-(0)} = (\kappa^-)^2 u_{2,2}^{-(0)}, \\ &\sigma_{12}^{-(0)} = u_{1,2}^{-(0)}, \end{aligned} \tag{4.9}$$

subject to

$$u_i^{-(0)}\big|_{\xi_2=0} = 0, \qquad u_i^{-(0)}\big|_{\xi_2=1} = v_i^*. \tag{4.10}$$

Then, we obtain from $(4.9)_3$

$$\sigma_{22}^{-(0)} = (\kappa^-)^2 \frac{\partial u_2^{-(0)}}{\partial \xi_2}. \tag{4.11}$$

Substituting (4.11) into $(4.9)_1$, we deduce a second order ordinary differential equation

$$\frac{\partial^2 u_2^{-(0)}}{\partial \xi_2^2} + \left(\frac{\Omega^-}{\kappa^-}\right)^2 u_2^{-(0)} = 0. \tag{4.12}$$

from which, satisfying the boundary conditions (4.10)

$$u_2^{-(0)} = \frac{v_2^*}{\sin\left(\dfrac{\Omega^-}{\kappa^-}\right)} \sin\left(\frac{\Omega^-}{\kappa^-}\xi_2\right). \tag{4.13}$$

Following the same procedure for $u_1^{-(0)}$, we get

$$u_1^{-(0)} = \frac{v_1^*}{\sin(\Omega^-)} \sin(\Omega^- \xi_2), \tag{4.14}$$

and, finally,

$$\sigma_{22}^{-(0)} = \frac{\kappa^- \Omega^- v_2^*}{\sin\left(\dfrac{\Omega^-}{\kappa^-}\right)} \cos\left(\frac{\Omega^-}{\kappa^-}\xi_2\right), \qquad \sigma_{12}^{-(0)} = \frac{\Omega^- v_1^*}{\sin(\Omega^-)} \cos(\Omega^- \xi_2). \tag{4.15}$$

It is underlined that the thickness variation for stresses (4.15) is not polynomial, but sinusoidal, which is characteristic of high-frequency long-wave approximations.

Due to continuity conditions $(2.4)_2$, in which $v_i = u_i^+$, the last expressions (4.15) taken at the lower face of the layer $\xi_2 = 1$ ($x_2 = 0$) lead to the sought for effective boundary conditions. In the dimensional variables they take the form ($x_2 = 0$)

$$\sigma_{22}^+ = \kappa^- \omega \sqrt{\rho^- \mu^-}\, u_2^+ \cot\left(\frac{\omega h}{c_2^- \kappa^-}\right), \qquad \sigma_{12}^+ = \omega \sqrt{\rho^- \mu^-}\, u_1^+ \cot\left(\frac{\omega h}{c_2^-}\right). \tag{4.16}$$

As might be expected, the derived conditions fail at

$$\sin\left(\frac{\omega h}{c_2^- \kappa^-}\right) = 0 \qquad \text{or} \qquad \sin\left(\frac{\omega h}{c_2^-}\right) = 0, \tag{4.17}$$

corresponding to thickness resonances (3.5). The asymptotic technique oriented to the vicinities of thickness resonances is presented in a number of publications, e.g. [16,32].

We also remark that in the low-frequency limit $\omega \to 0$ the effective boundary conditions (4.16), are simplified to a more traditional form

$$\sigma_{22}^{+} = \frac{\left(\kappa^{-}\right)^{2}\mu^{-}}{h}u_2^{+}, \qquad \sigma_{13}^{+} = \frac{\mu^{-}}{h}u_1^{+}, \tag{4.18}$$

not containing a frequency parameter.

5. Non-uniform asymptotics

Let us start from the hyperbolic equation (B.8) for the Rayleigh wave, in which, according to (4.16),

$$Q_1 = \frac{\kappa^{-}\mu^{-}}{h}\,\Omega^{-}\cot\left(\frac{\Omega^{-}}{\kappa^{-}}\right)u_2^{+}\big|_{x_2=0}, \qquad Q_2 = \frac{\mu^{-}}{h}\,\Omega^{-}\cot\left(\Omega^{-}\right)u_1^{+}\big|_{x_2=0}, \tag{5.1}$$

where, as above, we assume $\Omega^{-} \lesssim 1$. Within the framework of the explicit asymptotic model oriented to contribution of the Rayleigh wave only, exposed in Appendix B, see also [19] and references therein, the displacements in (5.1) may be expressed through the Lamé potential φ^{+} as

$$u_1^{+} = \frac{1-\beta_R^2}{2}\,\varphi_{,1}^{+}, \qquad u_2^{+} = -\frac{1-\beta_R^2}{1+\beta_R^2}\,\varphi_{,2}^{+} = \alpha_R\,\frac{1-\beta_R^2}{1+\beta_R^2}\,\mathcal{H}(\varphi_{,1}), \tag{5.2}$$

where $\mathcal{H}$ stands for the Hilbert transform

$$\mathcal{H}(f(x)) = \frac{1}{\pi}\,\mathrm{p.v.}\int_{-\infty}^{\infty}\frac{f(\xi)}{x-\xi}\,d\xi, \tag{5.3}$$

see e.g. [12], and α_R and β_R are given by (B.5).

Then, the time-harmonic form of (B.8) becomes (factor of $\mathrm{e}^{-i\omega t}$ is separated)

$$\varphi_{,11}^{+} + \frac{1}{c_R^2}\left(\frac{\Omega^{-}c_2^{-}}{h}\right)^{2}\varphi^{+} + \frac{\mu}{h}\,\Omega^{-}\gamma\mathcal{H}(\varphi_{,1}^{+}) = 0, \tag{5.4}$$

where

$$\gamma = \frac{\beta_R(\beta_R^2-1)\left[\left(1+\beta_R^2\right)^{2}\cot\left(\Omega^{-}\right) + 4\alpha_R^2\kappa^{-}\cot\left(\dfrac{\Omega^{-}}{\kappa^{-}}\right)\right]}{8\left[\beta_R^2 + \alpha_R^2(1-2\beta_R^2) + \alpha_R\beta_R(\beta_R^4-1)\right]}. \tag{5.5}$$

Thus, the earlier established equation for the Rayleigh wave on a homogeneous elastic half-space is now perturbed by an integral (or pseudo-differential) operator multiplied by the small parameter (2.5).

Let us investigate the dispersion relation corresponding to (5.4), at $\mu \ll 1$. Setting, $\varphi^{+} = \mathrm{e}^{ikx_1}$ $(k \geq 0)$, we have

$$\frac{\zeta^2}{\zeta_R^2} + \sqrt{\mu\rho}\gamma\zeta - 1 = 0, \tag{5.6}$$

with $\zeta = c/c_2^{+}$ and $\zeta_R = c_R/c_2^{+}$, where, as before, $c = \omega/k$ is the phase speed. This immediately gives $O(\sqrt{\mu})$ correction to the Rayleigh wave speed $\zeta = \zeta_R$, thus

$$\zeta = \zeta_R - \frac{1}{2}\sqrt{\mu\rho}\gamma\zeta_R^2 + \ldots. \tag{5.7}$$

This asymptotic formula is not uniformly valid, since $\gamma \to \infty$ at thickness resonances (3.5), and also at $\Omega^{-} \to 0$, when

$$\gamma = \frac{\beta_R(\beta_R^2-1)\left(1+2\beta_R^2+\beta_R^4+4\alpha_R^2\left(\kappa^{-}\right)^{2}\right)}{8\Omega^{-}\left[\beta_R^2 + \alpha_R^2(1-2\beta_R^2) + \alpha_R\beta_R(\beta_R^4-1)\right]}. \tag{5.8}$$

In this case, the low-frequency Rayleigh-type wave has a non-zero cut-off frequency, which is in agreement with numerical data in Figures 2 and 4. It is also obvious that the equation (5.7) with γ given by (5.8) would follow from the low-frequency effective boundary conditions (4.18).

In contrast to the consideration above, the low-frequency Rayleigh-type wave for a coated half-space with traction-free surface has no cut-off frequency. Indeed, it is governed by a singularly perturbed wave equation, see [10]

$$\Box_R \varphi^+ - bh\mathcal{H}(\varphi^+_{,111}) = 0, \tag{5.9}$$

where

$$\Box_R = \frac{\partial^2}{\partial x_1^2} - \frac{1}{c_R^2}\frac{\partial^2}{\partial t^2}, \tag{5.10}$$

is the d'Alembert operator, and the material constant b is defined by formula (4.23) in [10].

The associated dispersion relation is -

$$\frac{\zeta^2}{\zeta_R^2} + \frac{\sqrt{\mu}}{\sqrt{\rho}}\frac{b\Omega^-}{\zeta} - 1 = 0, \tag{5.11}$$

supporting the surface wave with $\zeta = \zeta_R$ at $\Omega^- = 0$.

6. Comparison with the exact solution

This section contains numerical study of the derived asymptotic approximation for the wave speed (5.7). The variation of the scaled phase velocity $\zeta = c/c_2^+$ on the dimensionless frequency Ω^+ is presented for both exact dispersion relation (2.12) and the approximation (5.7), for the material parameters (3.1), see Figures 5 a), b) illustrating the near-zero vicinity of the first mode and the high-frequency domain for $\mu = 0.001$. In these Figures, red dashed lines represent the asymptotic approximation (5.7), and blue solid curves correspond to the exact dispersion relation (2.12).

It is observed from Figure 5 a) that, as expected, in the vicinity of $\Omega^+ = 0$ approximation (5.7) is reasonably close to the exact solution in a narrow region only, associated with the first non-zero cut-off frequency. On the contrary, Figure 5 b) shows that for $\Omega^+ \sim 1$ the approximation (5.7) is valid over a remarkably broad range of frequencies, except for the cut-off frequencies, where the effective boundary conditions (4.16) fail.

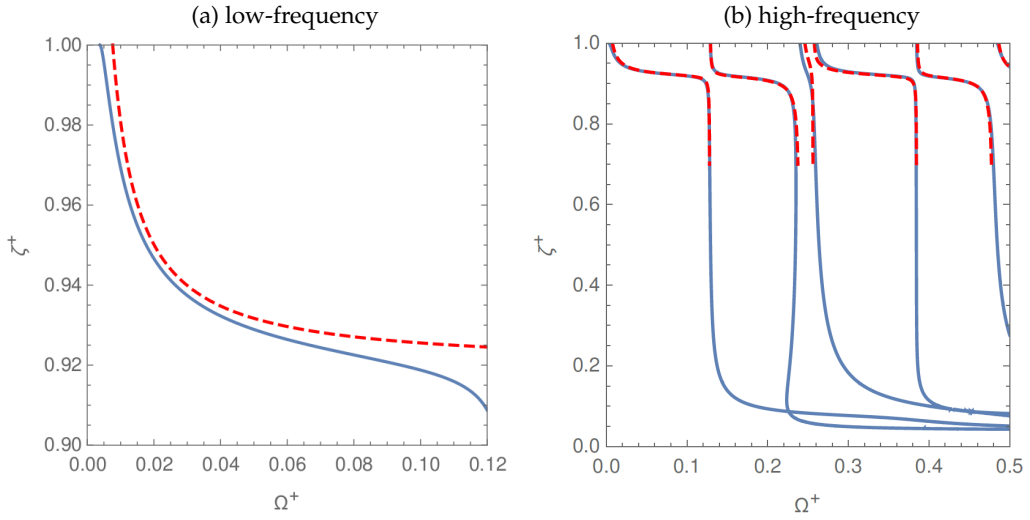

Figure 5. Rayleigh-type modes (2.12) and its approximation (5.7) for high contrast $\mu = 0.001$ over a) low-frequency region; b) high-frequency domain

7. Conclusion

The non-traditional effective boundary conditions (4.16) are derived using a long-wave high-frequency asymptotic procedure, e.g. see [16]. They incorporate the effect of a soft thin coating clamped along the surface, resulting in a regular operator perturbation of the equation governing the Rayleigh wave (5.4). It is interesting that the analogous conditions for a coating with a free surface in [10] lead to a singular perturbation, see also [19].

The non-uniform asymptotic formulae for the family of Rayleigh-type waves (5.7), deduced from the equation (5.4), fail in the vicinities of the thickness resonances (3.5) and zero frequency. In this case, in contrast to a coating with a traction-free surface, the lowest wave has a cut-off frequency, which is in line with the non-existence of surface waves on a clamped homogeneous half-space.

Of course, the aforementioned formulae (5.7) could be readily obtained from the original equations in linear elasticity (2.7) subject to the established effective conditions (4.16). However, the approach implemented above, originating from the approximate formulation for the Rayleigh-type wave (5.4) brings in a number of advantages. In particular, it allows various generalisations, including, in particular, taking into account external loading, 3D effects and transient phenomena, as it has been done for a homogeneous half-space, see [19].

It is also worth mentioning the useful findings in Section 3, including evaluation of zeros of the function F, facilitating interpretation of the numerical data calculated from the full dispersion relation (2.12). In this case, the similarity with more explicit results for Love-type waves, see Appendix A, is intensively exploited.

Finally, we note the phenomenon of the lowest cut-off frequency tending to zero in case of especially high contrast ($\mu \ll 1$), which is in line with vibrations of high-contrast elastic composites, see [20].

Appendix A. Love-type waves on a layered half-space with a clamped surface

Consider an anti-plane problem for a half-space ($x_2 \geq 0$) coated by a layer ($-h \leq x_2 \leq 0$), i.e. assume $u_1^{\pm} = u_2^{\pm} = 0$ and $u_3^{\pm} = u_3^{\pm}(x_1, x_2, t)$. This scalar problem of elasticity allows some qualitative insight into the dynamic response of a layered half-space with a clamped surface, having obvious parallels with the plane problem, see Section 3. The equations of anti-plane motion are given by

$$u_{3,11}^{\pm} + u_{3,22}^{\pm} = \frac{1}{(c_2^{\pm})^2} u_{3,tt}^{\pm}, \tag{A.1}$$

together with the constitutive relations

$$\sigma_{13}^{\pm} = \mu^{\pm} u_{3,1}^{\pm}, \qquad \sigma_{23}^{\pm} = \mu^{\pm} u_{3,2}^{\pm}. \tag{A.2}$$

The boundary condition modelling a clamped surface $x_2 = -h$ is taken as

$$u_2^{-} = 0. \tag{A.3}$$

The continuity conditions at the interface are given by

$$u_3^{-}\big|_{x_2=0} = u_3^{+}\big|_{x_2=0}, \qquad \sigma_{23}^{-}\big|_{x_2=0} = \sigma_{23}^{+}\big|_{x_2=0}. \tag{A.4}$$

The displacements satisfying (A.1) and the decay conditions are taken in the form

$$u_3^{-} = \Big(A_1 \cos(\beta^{-} k x_2) + A_2 \sin(\beta^{-} k x_2)\Big)\, \mathrm{e}^{ik(x_1 - ct)}, \qquad u_3^{+} = A_3 \mathrm{e}^{ik(x_1 - ct) - \beta^{+} k x_2}, \tag{A.5}$$

where A_n, $n = 1, 2, 3$ are arbitrary constants, and β^{-} and β^{+} are defined in (2.10) and (2.11), respectively. The associated dispersion relation may then be derived, giving

$$\tan(kh\beta^{-}) + \frac{\mu\beta^{-}}{\beta^{+}} = 0. \tag{A.6}$$

Numerical illustrations of the dispersion relation (A.6), showing the scaled frequency Ω^+ vs. the dimensionless wave number K, see (3.3), are presented in Figure 6 for several values of the relative stiffness $\mu = 0.1$, $\mu = 0.3$, and $\mu = 0.5$, with the material parameters (3.1). Here, the blue solid lines represent exact dispersion curves, yellow and green dashed lines correspond to the shear wave speeds of the substrate $c = c_2^+$ and the coating $c = c_2^-$, respectively.

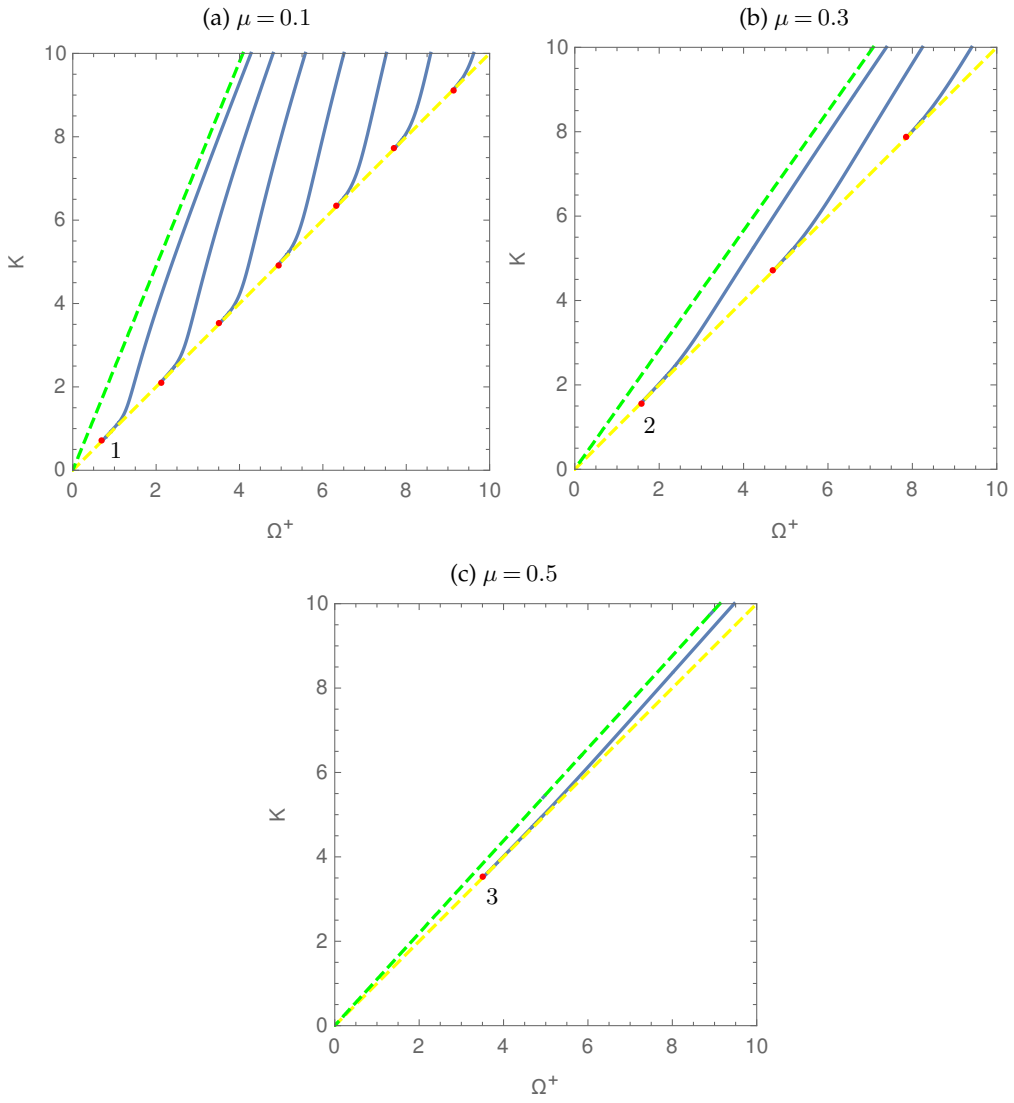

Figure 6. Dispersion curves for Love-type waves for several types of contrast (a) $\mu = 0.1$; (b) $\mu = 0.3$; (c) $\mu = 0.5$

Predictably, it is observed from Figure 6 that as the contrast becomes less noticeable (μ is getting closer to unity), the angle between the dashed lines depicting shear wave fronts of the layer and the half-space becomes narrower, with the solution of the dispersion relation (A.6) lying within this angle. This confirms a well-known fact that the Love waves exist provided that the shear wave speed of the half-space exceeds that of the layer, i.e. $c_2^- < c_2^+$, or $\mu < \rho$, with the same phenomena noted in the associated plane problem, see (3.2). Similarly to Rayleigh waves, in case of a homogeneous half-space ($\mu = 1$), dispersion relation (A.6) does not allow a localised solution.

The initial points of the dispersion modes (the cut-off frequencies) are located on the line $c = c_2^+$ or $\Omega^+ = K$ (denoted with red dots), see Figure 6. Therefore, as $\beta^+ \to 0$, it follows from (A.6) that $\tan(kh\beta^-) \to \infty$, hence, the expressions for the cut-off frequencies are given explicitly by

$$\Omega_0^+ = K_0 = \frac{\pi(2n-1)}{2\sqrt{\dfrac{\rho}{\mu} - 1}}, \qquad n = 1, 2, 3, \dots . \tag{A.7}$$

It is also worth noting that the value of the lowest cut-off frequency decreases with increase in contrast (as $\mu \to 0$), see points 1, 2, and 3 in Figure 6, which also follows (A.7).

On the other hand, in the limit $K \gg 1$, the phase velocity tends to the shear wave speed of the layer, i.e., $c \to c_2^-$, therefore, $\beta^- \to 0$. Hence, from (A.6), $\tan(kh\beta^-) \to 0$, implying

$$\Omega^+ \sim \sqrt{\frac{\mu(\pi^2 n^2 + K^2)}{\rho}}, \qquad n = 1, 2, 3, \dots, \qquad K \gg 1. \tag{A.8}$$

Thus, the consideration for Love-type waves in a coated half-space with a clamped surface clarifies the localised wave phenomena, giving explicit formulae for the cut-off frequencies and providing parallels with a less trivial plane-strain case, see Section 3.

Appendix B. Explicit asymptotic model for the Rayleigh wave

Consider plane-strain problem (2.7) for a homogeneous elastic half-space $x_2 \geq 0$ subject to the prescribed surface stresses

$$\sigma_{22}^+\big|_{x_2=0} = Q_1(x_1, t), \qquad \sigma_{12}^+\big|_{x_2=0} = Q_2(x_1, t). \tag{B.1}$$

In this case, the contribution of the Rayleigh wave expressed in terms of the Lamé potentials can be presented as a superposition

$$\varphi^+ = \varphi_1^+ + \varphi_2^+, \qquad \psi^+ = \psi_1^+ + \psi_2^+ \tag{B.2}$$

where, as shown in [19], see also references therein,

$$\Box_R \varphi_1^+\big|_{x_2=0} = \frac{1+\beta_R^2}{2\mu^+ B} Q_1, \qquad \Box_R \psi_2^+\big|_{x_2=0} = -\frac{1+\beta_R^2}{2\mu^+ B} Q_2, \tag{B.3}$$

where $\Box_R$ is the d'Alembert operator defined by (5.10),

$$B = \frac{\alpha_R}{\beta_R}(1-\beta_R^2) + \frac{\beta_R}{\alpha_R}(1-\alpha_R^2) - 1 + \beta_R^4, \tag{B.4}$$

with

$$\alpha_R = \sqrt{1 - \frac{c_R^2}{(c_1^+)^2}}, \qquad \beta_R = \sqrt{1 - \frac{c_R^2}{(c_2^+)^2}}. \tag{B.5}$$

The wave equations (B.3) may be transformed to a single one, using the identities

$$\psi^+ = \frac{2\alpha_R}{1+\beta_R^2}\mathcal{H}(\varphi^+), \qquad \varphi^+ = -\frac{2\beta_R}{1+\beta_R^2}\mathcal{H}(\psi^+), \tag{B.6}$$

see [7] and [19] for further detail, where $\mathcal{H}$ denotes the Hilbert transform. In particular, the second equation in (B.3) can be reduced to

$$\Box_R \varphi_2^+\big|_{x_2=0} = \frac{\beta_R}{\mu^+ B}\mathcal{H}(Q_2). \tag{B.7}$$

Finally, adding the first equation in (B.3) and (B.7), we arrive at

$$\Box_R \varphi^+ = \frac{1}{2\mu^+ B}\left[\left(1+\beta_R^2\right) Q_1 + 2\beta_R \mathcal{H}(Q_2)\right], \tag{B.8}$$

where, once again, $\Box_R$ is the d'Alembertian, see (5.10).

Authors' Contributions. All of the authors contributed equally to this manuscript.

Competing Interests. No competing interests to declare.

Funding. The research was not externally funded.

Acknowledgements. LS gratefully acknowledges the Keele University ACORN Scholarship.

References

1. Achenbach J. 1998. Explicit solutions for carrier waves supporting surface waves and plate waves. *Wave Motion*, **28**(1), 89–97.
2. Achenbach J. 2012. *Wave propagation in elastic solids*. Elsevier: Amsterdam.
3. Aghalovyan LA. 2015. *Asymptotic theory of anisotropic plates and shells*. World Scientific: Singapore.
4. Agalovyan LA, & Gulgazaryan, LG. 2006. Asymptotic solutions of non-classical boundary-value problems of the natural vibrations of orthotropic shells. *J. Appl. Math. Mech.* **70**(1), 102–115.
5. Agalovyan ML, & Zakaryan TV. (2019) Asymptotic solution of the first 3D dynamic elasticity theory problem on forced vibrations of a three-layer plate with an asymmetric structure. *Mech. Comp. Mat.* **55**(1), 3–18.
6. Babich VM, & Kiselev AP. 2018. *Elastic waves: high frequency theory*. Chapman and Hall/CRC: New York.
7. Chadwick P. 1976. Surface and interfacial waves of arbitrary form in isotropic elastic media. *J. Elast*, **6**(1), 73–80.
8. Cherednichenko KD, & Cooper S. 2015. On the existence of high-frequency boundary resonances in layered elastic media. *Proc. R. Soc. A* **471**(2178), 20140878.
9. Colombi A, Colquitt D, Roux P, Guenneau S, & Craster RV. 2016. A seismic metamaterial: The resonant metawedge. *Sci. Rep.* **6**, 27717.
10. Dai HH, Kaplunov J, & Prikazchikov DA. 2010. A long-wave model for the surface elastic wave in a coated half-space. *Proc. R. Soc. A* **466**(2122), 3097–3116.
11. Ege N, Erbaş B, Kaplunov J, & Wootton P. 2018. Approximate analysis of surface wave-structure interaction. *J. Mech. Mat. Struct.* **13**(3), 297–309.
12. Erdelyi A, Magnus W, Oberhettinger F, & Tricomi F. 1954. *Table of integral transforms (Vol. 2)*. McGraw-Hill: New York.
13. Friedlander F. 1948. On the total reflection of plane waves. *Quart. J. Mech. Appl. Math.*, **1**(1), 376–384.
14. Kaplunov JD. 1995. Long-wave vibrations of a thinwalled body with fixed faces. *Quart. J. Mech. Appl. Math.*, **48**(3), 311–327.
15. Kaplunov J, & Kossovich LY. 2004. Asymptotic model of Rayleigh waves in the far-field zone in an elastic half-plane. *Dokl. Phys.* **49**(4), 234–236.
16. Kaplunov J, Kossovich LY, & Nolde EV. 1998. *Dynamics of thin walled elastic bodies*. Academic Press: San Diego.
17. Kaplunov J, & Krynkin A. 2006. Resonance vibrations of an elastic interfacial layer. *J. Sound Vib.*, **294**, 663–677.
18. Kaplunov JD, & Markushevich DG. 1993. Plane vibrations and radiation of an elastic layer lying on a liquid half-space. *Wave Motion* **17**(3), 199–211.
19. Kaplunov J, & Prikazchikov DA. 2017. Asymptotic theory for Rayleigh and Rayleigh-type waves. *Adv. Appl. Mech.* **50** 1–106, Elsevier.
20. Kaplunov J, Prikazchikov DA, & Prikazchikova LA. 2017. Dispersion of elastic waves in a strongly inhomogeneous three-layered plate. *Int. J. Solids Struct.* **113**, 169–179.
21. Kaplunov J, Zakharov A, & Prikazchikov DA. 2006. Explicit models for elastic and piezoelastic surface waves. *IMA J. Appl. Math.*, **71**, 768–782.
22. Kiselev AP. 2004. Rayleigh wave with a transverse structure. *Proc. R. Soc. A* **460**(2050), 3059–3064.
23. Kiselev AP. 2015. General surface waves in layered anisotropic elastic structures. *Zapiski Nauchnykh Seminarov POMI* **438**, 133–137.
24. Kiselev AP & Parker DF. 2010. Omni-directional Rayleigh, Stoneley and Schölte waves with general time dependence. *Proc. R. Soc. A* **460**(2120), 2241âĂŞ2258.
25. Lashhab MI, Rogerson GA, & Prikazchikova LA. 2015. Small amplitude waves in a pre-stressed compressible elastic layer with one fixed and one free face. *ZAMP* **66**(5), 2741–2757.

26. Nobili A, & Prikazchikov DA. 2018. Explicit formulation for the Rayleigh wave field induced by surface stresses in an orthorhombic half-plane. *Europ. J. Mech. A* **70**, 86–94.
27. Nolde EV, & Rogerson GA. 2002. Long wave asymptotic integration of the governing equations for a pre-stressed incompressible elastic layer with fixed faces. *Wave motion* **36**(3), 287–304.
28. Parker DF. 2013. The Stroh formalism for elastic surface waves of general profile. *Proc. R. Soc. A* **469**(2160), 20130301.
29. Parker DF, & Kiselev AP. 2008. Rayleigh waves having generalised lateral dependence. *Quart. J. Mech. Appl. Math.* **62**(1), 19–30.
30. Prikazchikov DA. 2013. Rayleigh waves of arbitrary profile in anisotropic media. *Mech. Res. Comm.* **50**, 83–86.
31. Rayleigh L. 1885. On waves propagated along the plane surface of an elastic solid. *Proc. Lond. Math. Soc.* **1**(1), 4–11.
32. Rogerson GA, Sandiford KJ, & Prikazchikova LA. 2007. Abnormal long wave dispersion phenomena in a slightly compressible elastic plate with non-classical boundary conditions. *Int. J. Non-Linear Mech.* **42**(2), 298–309.
33. Rousseau M, & Maugin GA. 2010. Rayleigh surface waves and their canonically associated quasi-particles. *Proc. R. Soc. A* **467**(2126), 495–507.
34. Slepyan LI. 2012. *Models and phenomena in fracture mechanics*. Springer Science & Business Media: Berlin.
35. Sobolev SL. 1937. Some problems in wave propagation. In P. Frank & R. von Mises (Eds.), *Differential and integral equations of mathematical physics*. Moscow-Leningrad, ONTI, 468–617.
36. Tiersten HF. 1969. Elastic surface waves guided by thin films. *J. Appl. Phys.* **40**, 770–789.
37. Vinh PC, & Linh NTK. 2012. An approximate secular equation of Rayleigh waves propagating in an orthotropic elastic half-space coated by a thin orthotropic elastic layer. *Wave Motion* **49**(7), 681–689.
38. Vinh PC, Anh VTN, & Thanh VP. 2014. Rayleigh waves in an isotropic elastic half-space coated by a thin isotropic elastic layer with smooth contact. *Wave Motion* **51**(3), 496–504.